



# The Structure and Properties of a-C:Ti and a-C:Ti:N Coatings Deposited on a Titanium and Titanium Nitride Sublayer

Xiaohong Jiang<sup>1</sup> , Dzmitry Piliptsou<sup>1,2</sup> ,  
Aliaksandr Rogachev<sup>1,2</sup> , Ekaterina Kulesh<sup>1,2</sup>, and Yiming Liu<sup>1,2</sup>

<sup>1</sup> International Chinese-Belarusian Scientific Laboratory by Vacuum-Plasma Technologies, Nanjing University of Science and Technology, 200, Xiaolingwei street, Nanjing 210094, China  
jiangxh24@njjust.edu.cn

<sup>2</sup> Francisk Skorina Gomel State University, 104, Sovetskaya St., 246019 Gomel, Belarus

**Abstract.** This paper presents the deposition of Ti(TiN)/a-C:Ti(TiN) coatings, doped by titanium and nitrogen atoms on steel 316L and Si substrates, to study the microstructures and mechanical properties. The coatings were obtained using titanium cathode DC and graphite target pulse arc sputtering under nitrogen pressure of  $10^{-1}$  Pa. The phase composition in the coatings was studied by XPS and Raman spectroscopy. XPS results showed that Ti-C bonds formed in the Ti/TiN/a-C:Ti coating, while Ti-N, Ti-C, C-N bonds were observed in the Ti/TiN/a-C:Ti:N coatings. Raman spectroscopy exhibited that the doped titanium layers into a-C coatings decrease the size of  $Csp^2$  clusters. An increased disordering was also observed in  $Csp^2$  clusters, which is essential for the mechanical properties. The surface microstructure of the coatings was further characterized by AFM, which indicated strong dependences on the droplet phase, grain size, and nature (such as graphite, titanium carbide, titanium carbonitride) the coating. The microhardness of coatings rose to 12.5 GPa. The doped titanium layers decreased internal stresses in Ti/TiN/a-C:Ti, i.e., 108,1 MPa. The friction coefficient is less than 0.3, dependent on the presence of Ti atoms in a-C coatings. Internal stresses are reduced due to the introduction of doping elements and soft metal layers in the coating structure. The change in the  $sp^2/sp^3$  ratio determines the change in microhardness values and kinetics of friction.

**Keywords:** Multilayer carbon coatings · Titanium · Nitrides · XPS · Spectroscopy · Structure · Morphology · Friction · Microhardness

## 1 Introduction

Modern ion-plasma technologies make it possible to deposit protective coatings of various stoichiometric and chemical compositions on the functional surfaces of the cutting tool and various structural elements of machine parts [1, 2]. The thin-film hardening technology consists of the fact that coatings with a thickness of several nanometers to several micrometers are deposited on the working surfaces of assembly parts subjected to increased loads. These coatings provide an increase in the service life. The a-C coatings containing carbon clusters with different hybridization of bonds are characterized by an exceptional combination of physical and mechanical properties. As noted in previous papers on this topic [3, 4, 6, 7], the main variable parameters of multilayer coatings based on solid layers are the thickness values, the nature, and the arrangement of individual layers involved in forming a given structure. A considerable number of papers have been devoted to the peculiarities of the properties of multilayer coatings based on thin layers, and there are theoretical approaches to choosing the optimal geometric parameters of a multilayer structure. However, there are a lot of aspects considering multilayer carbon-containing coatings that remain unclear, including the influence of the nature and parameters of the metal or nitride layer on the structure and properties of the carbon-based upper layer. A structural feature of such coatings is a high proportion of interphase interfaces relative to the total volume of interfaces, which significantly affect the properties of the multilayer coating. The grain boundaries are areas with high compositional heterogeneity. They contain structural defects, which, in particular, are obstacles to the propagation of dislocations and cracks, which implies an increase in the hardness of the coatings and a decrease in internal stresses.

The formation of nanostructured layered coatings with high mechanical properties is possible through a particular selection of conditions and deposition modes, coating design parameters, and the analysis and study of interphase interaction processes. The resulting coatings of the given composition and structure with stable performance properties, resistant to multifactorial operating conditions, are impossible without analyzing the features of the coating structure formation process.

The presence of the metal coating and/or metal nitride in the Me(MeN)/a-C:Me(MeN) structure makes it possible to increase the strength of the adhesive bond between the coating and the substrate, and also to reduce the level of internal stresses due to the plasticity of the metal layers [5, 6]. The application of such coatings is limited by the deposition and growth features, catalytic and chemical processes of interaction between elements in the coating, leading to a change in the structure and, consequently, in mechanical properties.

Mechanical properties (microhardness, internal stresses, friction, and wear resistance) of coatings containing layers of metals or nitrides Me(MeN)/a-C:Me(MeN) depend and are determined by the presence and thickness of titanium (titanium nitride) layers and carbon layers doped with titanium and/or nitrogen [7]. Among the metals used to create composite carbon coatings, titanium is one of the most common elements caused by its ability to interact intensively with carbon to form titanium carbide, which is characterized by high hardness and toughness. The formation of titanium carbide

phases in the volume of the carbon matrix leads to a decrease in the propagation of dislocations in the coating volume, which causes a decrease in the growth of cracks in the contact interaction process, and due to the alternation of the phases “carbon” - “titanium carbide”, the coating retains high hardness at lower values of internal stresses [8].

This paper aims at determining the influence of technological conditions and synthesis modes of multilayer a-C:Ti and a-C:Ti:N coatings, deposited on a titanium and titanium nitride bilayer, on their structure, morphology, and mechanical properties.

## 2 Research Methodology

The Ti(TiN)/a-C:Ti(TiN) coatings were deposited on monocrystalline silicon wafers (111) and 3261 stainless steel substrates using a combined evaporation method that combines the evaporation of a titanium cathode by a DC arc (discharge current 70 A, titanium VT-100) and a graphite target by a pulsed arc discharge ( $f = 15$  Hz,  $U_{\text{pulse}} = 350$  V). The nitrogen partial pressure was  $10^{-1}$  Pa. The thickness of the coatings was  $(450 \pm 10)$  nm. The thickness of TiN layers did not exceed 150 nm. The thickness of Ti layers did not exceed 20 nm. The choice of previously sequentially deposited layers of titanium and titanium nitride as a sublayer makes it possible to ensure high strength of the adhesive bond of the multilayer coating with the substrate and individual layers between themselves [9].

The morphology of the coating surface was studied by atomic force microscopy (AFM) in the modes of topography and phase contrast measurement (scanning area  $3 \times 3 \mu\text{m}$ ) using a Solver-PRO P47 (NT-MDT).

Raman spectra were recorded using a Senterra Raman microscope (Bruker). The spectra were recorded in the spectral range of  $600 \div 2500 \text{ cm}^{-1}$ . The spectra were excited by radiation with a wavelength of 532 nm and a power of 20 mW.

The chemical composition and structure of carbon bonds were determined by the X-ray photoelectron spectroscopy (XPS) method during the substance excitation by  $K\alpha$ -radiation of aluminum with quantum energy of 1486.6 eV and total power of 25 W (PHI Quantera).

The wear tests were carried out according to the “sphere-plane” scheme (UMT 2-EC, Bruker). The  $\text{Si}_3\text{N}_4$  ball with a diameter of 5/32” was used as a counterbody.

Friction was carried out at a load of 0.5 N and a sliding speed of 0.1 m/s in an air environment at a relative humidity  $(42 \div 45)\%$  and a temperature of 22 °C. The contact pressure, Hertz calculated, was equal to 478.6 MPa.

Internal stress ( $\sigma$ ) in the coatings was determined using the Stoney formula considering the change in the curvature radius of the silicon substrate before and after the deposition of the coatings (Profiler Dektak XT, Bruker) [10].

The microhardness of the coatings was determined by the Knoop method in 15 different places on the coating surface, and the average value was determined on the basis of the results. The test load and duration were 245 mN and 10 s, respectively. Since the thickness of the coatings did not exceed  $1 \mu\text{m}$ , the obtained microhardness values were interpreted as the mechanical characteristic of the entire “coating-substrate” system.

### 3 Results

The concentration of elements in the surface layer of the coating was determined using the XPS (Table 1).

**Table 1.** The atomic concentration of the elements in the coating

Coating	C, at. %	O, at. %	N, at. %	Ti2p3, at. %
Ti/TiN/a-C	89.6	8.6	1.5	0.3
Ti/TiN/a-C:Ti	86.8	8.8	1.2	3.2
Ti/TiN/a-C:Ti:N	64.5	19.6	9.0	6.9

As can be seen, the coating contains nitrogen, oxygen, titanium, and carbon. Regardless of the deposition method of the upper layer, traces of titanium and nitrogen were found in the coating (presumably the reflexes from the underlying layers). Oxygen in the coating is present as a result of titanium oxidation in the residual atmosphere of the vacuum chamber or as a result of attachment to carbon after depressurization of the vacuum chamber. The presence of titanium and nitrogen is explained by diffusion processes and the coating of sufficiently large titanium particles formed at the deposition stage of Ti or TiN layers.

Figure 1 shows the spectra of C1s states of carbon atoms in the coatings deposited on layers of different nature. The C1s spectrum of the Ti/TiN/a-C coating (Fig. 1a) contains the peaks characteristic of  $Csp^2$  (peak at 284.3 eV),  $Csp^3$  (peak at 285.2 eV), and C–O bonds. Similar peaks (Fig. 1b, c) are also present in the spectra of the Ti/TiN/a-C:Ti and Ti/TiN/a-C:TiN coatings [11]. Some bonds determine the interaction of the Ti–N, Ti–C type in the spectra of Ti/TiN/a-C:Ti and Ti/TiN/a-C:TiN coatings. The presence of these connections is determined by the formation processes of the upper composite layer. The peak characterizing the Ti–C type interaction appears insignificantly in the spectrum of the C1s state of carbon atoms.

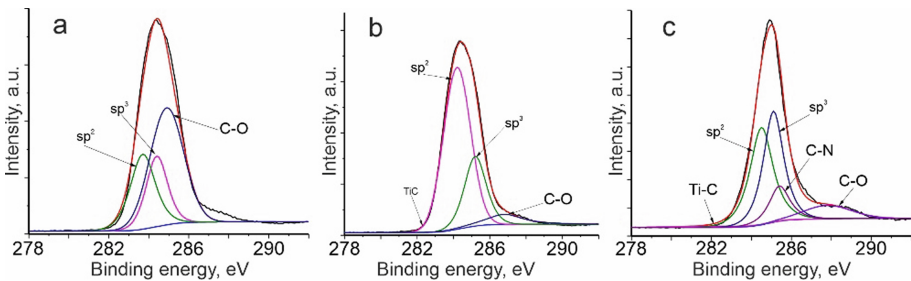


**Fig. 1.** XPS spectra of C1s peak: a – Ti/TiN/a-C, b – Ti/TiN/a-C:Ti, c – Ti/TiN/a-C:Ti:N

Figure 1(c) shows that doping carbon coatings with titanium and nitrogen leads to an increase in the intensity of the  $Csp^3$  component and a decrease in the  $Csp^2$  intensity,

which is consistent with the data in [12]. Comparing the ratios of the contributions of the integral areas of the  $Csp^2/Csp^3$  components for the coatings of different architectures, it can be concluded that binary doping with titanium and nitrogen causes a decrease in the content of carbon-carbon bonds due to the formation of chemical compounds of a different type, CN for example.

Figure 2(b) shows the spectrum of the  $Ti2p3$  state for the Ti/TiN/a-C:Ti:N coating. The  $Ti2p3$  spectrum contains peaks characteristic of chemical bonds such as Ti-O, Ti-N, and metallic titanium. The position and shape of the peak located at 457.8 eV characterize the Ti-CN type's bond and are in agreement with the data given in [6]. When the spectrum was decomposed into components, the peak characterizing the bond of the Ti-C type was not detected, which, according to the data given in [7], is associated with a low titanium concentration in the surface layer of the coating.

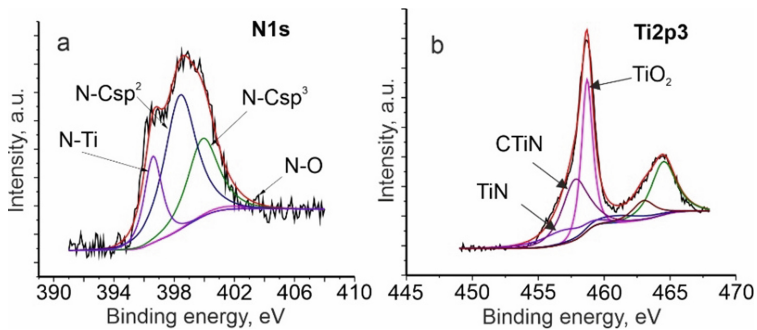


**Fig. 2.** N1s and  $Ti2p3$  XPS spectra of the Ti/TiN/a-C:Ti:N coatings

The low content of titanium in the form of carbide can be explained by the higher chemical activity of titanium and nitrogen than titanium and carbon, as well as by the bombardment of the growing coating with high-energy metal ions, which leads to the destruction of Ti-C bonds [13].

In the spectrum fragment corresponding to the N1s peak (see Fig. 2a), four peaks can be distinguished, localized on the energy scale at  $(396.0 \pm 0.2)$  eV,  $(398.7 \div 399.1)$  eV,  $(399, 5 \div 400.2)$  eV and  $(402.0 \pm 0.2)$  eV. Three dominant peaks located at 396.0, 398.7, and 400.2 eV are attributed to nitrogen chemically bonded to carbon in the states of  $Csp^2$ -,  $Csp^3$ -hybridization, and also characterize the interaction of the N-Ti type. The fourth peak corresponds to the N-O bond or carbon bonds [14].

The  $Csp^2/Csp^3$  ratio is 2.76 for the Ti/TiN/a-C coating, while the value of the  $Csp^2/Csp^3$  ratio decreases to 1.68 for the Ti/TiN/a-C:Ti coating. There is a further decrease in the  $Csp^2/Csp^3$  ratio to values of 1.01 for the Ti/TiN/a-C:Ti:N coatings. Based on these data, the introduction of titanium and nitrogen (along with the presence of nitride sublayers) leads to a decrease in the  $Csp^2/Csp^3$  ratio. Thus, the introduction of Ti and N into the coating structure causes an increase in the number of carbon atoms in the state with  $sp^3$ -hybridization of bonds compared to undoped and doped only with titanium, which is typical for the coating with a high content of the diamond phase. This

behavior of  $Csp^2/Csp^3$  is in close agreement with the data obtained by Raman spectroscopy and is confirmed by the results presented in [15, 16].

It is known [17] that the ratio of integrated intensities  $I_D/I_G$  determines the relative abundance of carbon atoms with  $sp^2$  and  $sp^3$  bond hybridization, while the position and width of the G peak determine the change in the size and degree of ordering of carbon  $Csp^2$  clusters. Depending on the deposition mode, the presence of titanium/titanium nitride layers, and titanium or nitrogen atoms in the upper carbon layer, the decomposition parameters of the Raman spectra change (Table 2). When titanium and titanium nitride are introduced into the carbon coating, the  $I_D/I_G$  ratio increases, which is caused by an increase in the number of carbon atoms in the state with  $sp^2$  bond hybridization and the formation of CN or CN/CTi/TiN bonds. This, in turn, leads to a decrease in the size of  $Csp^2$  carbon clusters and is characterized by an increase in the G-peak width compared to the Ti/TiN/a-C coating. The change in the degree of disordering of  $Csp^2$  clusters is ambiguous. In Ti/TiN/a-C:Ti coatings, the degree of ordering of carbon clusters increases. The subsequent introduction of nitrogen results in the formation of titanium nitride phases in the coating. This leads to a decrease in the degree of ordering of the carbon matrix, and is confirmed by the shift of the G peak position to the low wavenumbers region. Thus, the introduction of nitrogen or nitrogen/titanium atoms causes an increase in the ordering of carbon clusters compared to the coating containing the a-C layer [18].

As can be seen from the AFM images shown in Fig. 3, there are single drops with a size of at least 500 nm on the coating surface. Dispersion of the surface structure of the composite coatings depends on the nature of doping elements [14].

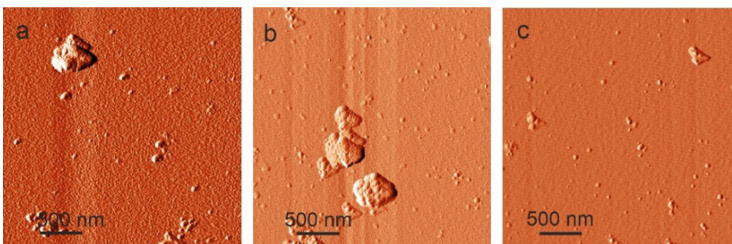


**Fig. 3.** AFM images of the surface of the coatings: a – Ti/TiN/a-C, b – Ti/TiN/a-C:Ti, c – Ti/TiN/a-C:Ti:N

The results of mathematical processing of the AFM images (see Fig. 3) are shown in Table 2.

**Table 2.** Statistical processing of AFM results

Coating	Ra, nm	D, nm	$I_D/I_G$ ratio	G peak width, $cm^{-1}$	G peak position, $cm^{-1}$
Ti/TiN/a-C:Ti:N	0.6	13.4	1.63	162.4	1567.2
Ti/TiN/a-C:Ti	3.3	18.5	1.64	150.6	1573.1
Ti/TiN/a-C	2.2	19.8	0.66	182.5	1563.5

It has been found that the nature of the doping element affects the coating roughness and grain size. Simultaneous doping with titanium and nitrogen allows a directed change in the grain size and, consequently, control of the parameters of the roughness of the layer [19]. The Ti/TiN/a-C:Ti:N coatings are characterized by the smallest roughness Ra and the smallest grain size D. The Ti/TiN/a-C:Ti coatings are characterized by the highest roughness, and the grain size is comparable to the undoped carbon layer. The surface morphology is determined by the titanium and carbon interaction and the formation of titanium carbide phases and a change in the size of the carbon cluster.

The wear tests showed that the friction kinetics of the Ti/TiN/aC:Ti:N coatings (Fig. 4 and Table 3) differs from the kinetic friction curves, obtained for other coatings by higher values of the friction coefficient and the wear coefficient of the counterbody, as well as by a small running-in area at the initial friction modes (Fig. 4) [20]. The Ti/TiN/a-C:Ti and Ti/TiN/a-C coatings retain their performance during the entire test period and are characterized by lower friction and wear coefficient (Table 3).

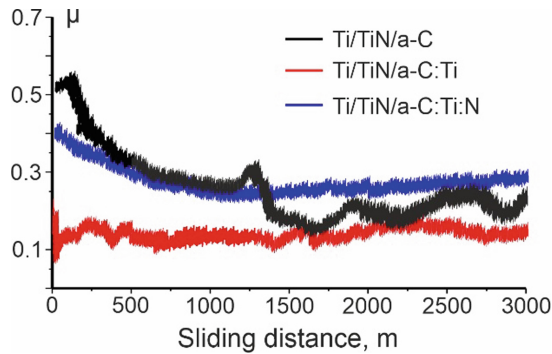


**Fig. 4.** Kinetic friction curves of the coatings containing titanium and titanium nitride bilayer

The main factors leading to such changes are changes in the strength of the adhesive joint due to the formation of the Ti sublayer. In this case, the formation of Ti or TiN layers leads to the redistribution of residual stresses between layers in the coating. An increase in their plasticity is also due to the formation of the structure containing boundary heterophase layers of a diffusion nature and an increase in the wear resistance of the coating or counterbody due to the presence of the coating graphite component in the coating surface layer [21]. As shown in Table 3, the microhardness of the coatings is determined by the presence of Ti and TiN layers and titanium in the diamond-like carbon layer. When nitrogen is introduced into the a-C:Ti coating structure, the microhardness is increased to 11.3 GPa. According to XPS data, this is determined by the formation of the TiN phase [22].

**Table 3.** Mechanical properties of the coatings containing layers of nitride nature

Coating	Hk, GPa	$\sigma$ , MPa	f	$j \times 10^{-11}$ , $m^3/(N \times m)$
Ti/TiN/a-C	12.5	167.8	0.29	2.4
Ti/TiN/a-C:Ti:N	11.3	116.3	0.21	10.1
Ti/TiN/a-C:Ti	10.5	108.1	0.14	7.2

It is shown (Table 3) that the formation of the a-C coatings doped with titanium or titanium and nitrogen leads to a decrease in internal stresses. Internal stresses are also reduced due to the content of titanium and titanium nitride layers in the coating structure [23]:

- 1 The Ti/TiN sublayer helps to reduce the effects caused by the difference in the thermal expansion coefficients of the substrate and the coating, which leads to a decrease in stresses in the surface carbon layer.
- 2 The upper layer of the a-C:Ti coating is dominated by bonds characteristic of titanium carbide and titanium metallic phase formation. Inclusions with a crystalline structure are formed in the amorphous carbon matrix, which makes it possible to reduce structural defects due to the alternation of  $sp^2$  and  $sp^3$  regions.

## 4 Conclusions

The XPS method has shown that the coating contains the Ti-C compounds. They are formed for the coatings with Ti and Ti-N, and Ti-C, CN compounds, which are formed for the coatings with Ti and N. Raman spectroscopy has shown that the introduction of titanium layers into the a-C coating leads to a decrease in the size of  $Csp^2$  clusters and an increase in the coating structure's disorder degree. The change in the  $sp^2/sp^3$  ratio determines the change in microhardness values and kinetics of friction.

AFM has shown the influence of the location of titanium or titanium nitride layers and the type of the alloying element on the surface morphology ( $R_a = 0,6$  nm for the Ti/TiN/aC:TiN coating, and for the Ti/TiN/a-C:Ti  $R_a = 3,6$  nm).

The carbon component of the coating is characterized by a high concentration of carbon atoms in the state of  $sp^3$  bond hybridization, as well as a low degree of ordering of carbon clusters, which causes an increase in internal stresses due to the formation of the structure with excessive boundary defects [24]. In coatings of the Ti/TiN/aC:Ti:N and Ti/TiN/aC:Ti type, the  $Csp^3$  bonds decrease due to the formation of carbides and carbonitride compounds in the coating structure, which, together with the presence of titanium and titanium nitride sublayers, leads to reduction of internal stresses.

The development of methods for separating plasma flows can be chosen as advanced research directions, i.e., removing microparticles from the plasma flow. Furthermore, the development of deposition technological methods and techniques allowing the formation of carbide/carbon coatings with a minimum content of metal that is chemically unbound with carbon, i.e., the coating consists of two interconnected matrices: carbide and carbon. By varying the ratio of carbide and carbon bonds in the

coating, it is possible to obtain a coating characterized by a polymatrix structure, representing compounds based on carbides/nitrides and diamond-like compounds.

**Acknowledgments.** Intergovernmental Cooperation Projects supported this work within the National Key Research and Development Plan of the Ministry of Science and Technology of PRC (projects No. 2016YFE0111800, for 2016–2019), and the Ministry of Education of the Republic of Belarus (assignment “Multiphase carbide/carbon coatings for friction units operating under high contact loads”).

## References

1. Xiao, S., et al.: Tin repellence on wave-soldering stainless steel holders coated with Ti/TiC/DLC. *Surf. Coat. Technol.* **320**, 614–618 (2016)
2. Zhou, B., et al.: Structure and optical properties of Cu-DLC composite films deposited by cathode arc with double-excitation source. *Diam. Relat. Mater.* **69**, 191–197 (2016)
3. Dai, M.-J., et al.: A study on metal-doped diamond-like carbon film synthesized by ion source and sputtering technique. *Plasma Process. Polym.* **4**, 215–219 (2007)
4. Martínez-Martínez, D., López-Cartés, C., Gago, R., Fernández, A., Sánchez-López, J.C.: Thermal stability and oxidation resistance of nanocomposite TiC/a-C protective coatings. *Plasma Process. Polym.* **6**, 462–467 (2009)
5. Kolesnyk, V., Peterka, J., Kuruc, M., Šimna, V., Moravčíková, J., Vopát, T., Lisovenko, D.: Experimental study of drilling temperature, geometrical errors and thermal expansion of drill on hole accuracy when drilling CFRP/Ti alloy stacks. *Materials* **13**(14), 32321–323217 (2020)
6. Zhou, B., et al.: Synthesis and characterization of Ti and N binary-doped  $\alpha$ -C films deposited by pulse cathode arc with ionic source assistant. *Surf. Interface Anal.* **50**, 506–516 (2018)
7. Ming, M.Y., et al.: Structure, mechanical and tribological properties of Ti-doped amorphous carbon films simultaneously deposited by magnetron sputtering and pulse cathodic arc. *Diam. Relat. Mater.* **77**, 1–9 (2017)
8. Liu, D.G., Tu, J.P., Hong, C.F., Gu, C.D., Mai, Y.J., Chen, R.: Improving mechanical properties of a-CN<sub>x</sub> films by Ti–TiN/CN<sub>x</sub> gradient multilayer. *Appl. Surf. Sci.* **257**, 487–494 (2010)
9. Castillo, H.A., Restrepo-Parra, E., Arango-Arango, P.J.: Chemical and morphological difference between TiN/DLC and  $\alpha$ -C: H/DLC grown by pulsed vacuum arc techniques. *Appl. Surf. Sci.* **257**, 2665–2668 (2011)
10. Stoney, G.G.: The tension of metallic films deposited by electrolysis. *Proc. Roy. Soc. A Math. Phys. Eng. Sci.* **82**(553), 172–175 (1909)
11. Lin, Y., Zia, A.W., Zhou, Z., Shum, P.W., Li, K.Y.: Development of diamond-like carbon (DLC) coatings with alternate soft and hard multilayer architecture for enhancing wear performance at high contact stress. *Surf. Coat. Technol.* **320**, 7–12 (2017)
12. Matsuoka, M., et al.: X-ray photoelectron spectroscopy and Raman spectroscopy studies on thin carbon nitride films deposited by reactive RF magnetron sputtering. *World J. Nano Sci. Eng.* **2**, 92–102 (2012)
13. Ferrari, A.C., Robertson, J.: Interpretation of Raman spectra of disordered and amorphous carbon. *Phys. Rev. B* **61**, 4095–4107 (2000)
14. Igartua, A., et al.: Screening of diamond-like carbon coatings in search of a prospective solid lubricant suitable for both atmosphere and high vacuum applications. *Tribiol. Int.* **114**, 192–200 (2017)

15. Boubiche, N., et al.: Kinetics of graphitization of thin diamond-like carbon (DLC) films catalyzed by transition metal. *Diam. Relat. Mater.* **9**, 190–198 (2019)
16. Huang, L., Yuan, J., Li, C., Hong, D.: Microstructure, tribological and cutting performance of Ti-DLC/ $\alpha$ -C: H multilayer film on cemented carbide. *Surf. Coat. Technol.* **353**, 163–170 (2018)
17. Babak, V.P., Bilchuk, Y.Y., Shchepetov, V.V.: Increased wear coatings due intrastructural self-correction. *J. Eng. Sci.* **6**(1), C11–C15 (2019)
18. Tyagi, A., Walia, R.S., Murtaza, Q., Pandey, S.M., Tyagi, P.K., Bajaj, B.: A critical review of diamond like carbon coating for wear resistance applications. *Int. J. Refract. Metal. Hard Mater.* **78**, 107–122 (2019)
19. Pillari, L.K., Umasankar, V., Sarma, A., Gupta, M.: DLC coating of magnesium nanocomposites using RF sputtering. *Mater. Today Proc.* **4**, 6737–6742 (2017)
20. Zarei Moghadam, R., Ehsani, M.H., Rezagholipour Dizaji, H., Kameli, P., Jannesari, M.: Modification of hydrophobicity properties of diamond like carbon films using glancing angle deposition method. *Mater. Lett.* **220**, 301–304 (2018)
21. Kano, M.: Overview of DLC-coated engine components. In: Cha, S.C., Erdemir, A. (eds.) *Coating Technology for Vehicle Applications*, pp. 37–62. Springer, Cham (2015). [https://doi.org/10.1007/978-3-319-14771-0\\_3](https://doi.org/10.1007/978-3-319-14771-0_3)
22. Vetter, J.: 60 years of DLC coatings: Historical highlights and technical review of cathodic arc processes to synthesize various DLC types, and their evolution for industrial applications. *Surf. Coat. Technol.* **257**, 213–240 (2014)
23. Bewilogua, K., Hofmann, D.: History of diamond-like carbon films - from first experiments to worldwide applications. *Surf. Coat. Technol.* **242**, 214–225 (2014)
24. Batory, D.A., Stanishevsky, A., Kaczorowski, W.: The effect of deposition parameters on the properties of gradient  $\alpha$ -C:H/Ti layers. *J. Achiev. Mater. Manuf. Eng.* **37**, 381–386 (2009)